Bio-Based Aerogels from Potato Residues for Glycine Storage and Controlled Release

Mariel A. Zevallos Luna,[a,b] Damase P. Khasa [b], and Véronic Landry [a,*]

* *Corresponding author: veronic.landry@sbs.ulaval.ca*

DOI: 10.15376/biores.21.1.580-605

GRAPHICAL ABSTRACT

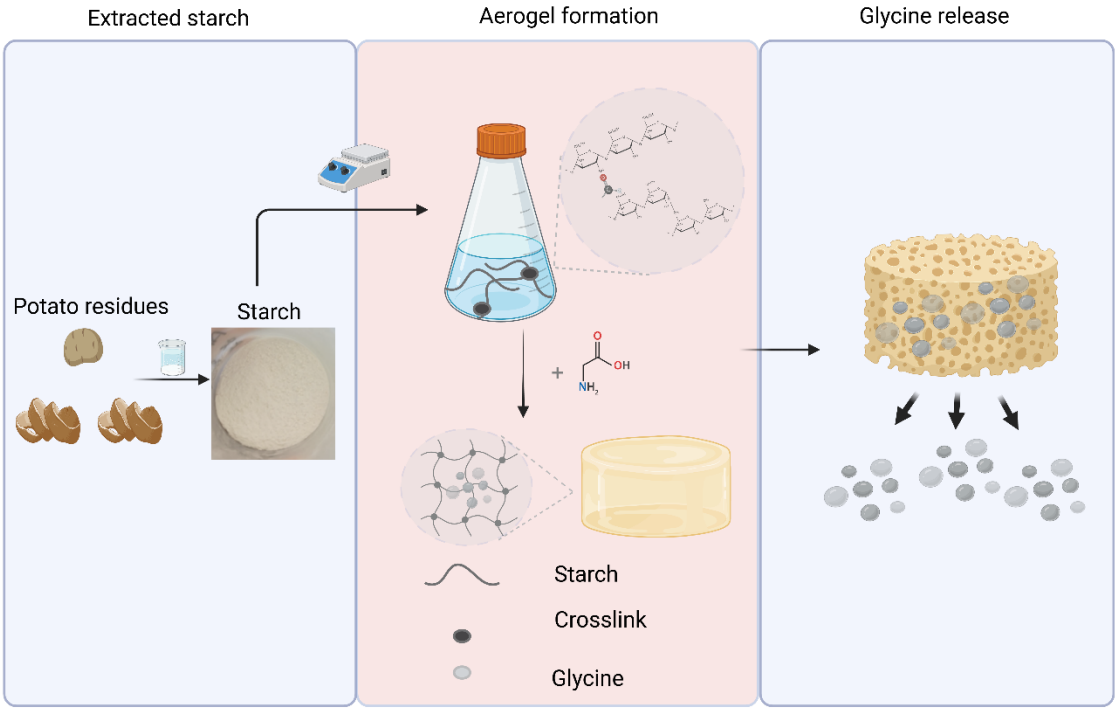

Bio-Based Aerogels from Potato Residues for Glycine Storage and Controlled Release

Mariel A. Zevallos Luna,[a,b] Damase P. Khasa [b] and Véronic Landry [a,*]

Biobased aerogels derived from starch offer a promising pathway for developing sustainable biomaterials. This study examines the use of starch extracted from potato peels to develop aerogels intended for glycine storage and controlled release. The reaction of starch with glutaraldehyde, used as a crosslinker, was demonstrated using Fourier-transform infrared spectroscopy, revealing the formation of hemiacetal bonds. Crosslinking enhanced thermal stability of the aerogels, as shown by thermogravimetric analysis, and improved their resistance to disintegration upon hydration. Glycine, an essential amino acid with agricultural and industrial applications, was loaded into the aerogels, and the release kinetics were evaluated under controlled conditions. Moreover, glycine acts as a neutralizing agent for residual glutaraldehyde, ensuring the suitability of the aerogel for applications where glutaraldehyde toxicity could be a concern. Structural characterization through scanning electron microscopy confirmed the porous architecture of the aerogels and revealed the presence of glycine crystals within the pores. These findings underscore the potential of crosslinked starch aerogels as eco-friendly carriers for bioactive molecules, paving the way for their application in agriculture and other fields.

DOI: 10.15376/biores.21.1.580-605

Keywords: Bio-based aerogels; Potato peel starch; Glutaraldehyde; Glycine; Controlled release; Agriculture application

Contact information: a: Department of Wood and Forest Sciences, Renewable Materials Research Centre, Université Laval, 2405 Rue de la Terrasse, Quebec City, Canada, G1V 0A6; b: Centre for Forest studies (CEF) and Institute for Integrative and Systemes Biology (IBIS), Department of Wood and Forest Sciences, Université Laval, 2405 Rue de la Terrasse, Quebec City, Canada, G1V 0A6;
** Corresponding author: veronic.landry@sbs.ulaval.ca*

INTRODUCTION

Aerogels are solid materials with a three-dimensional, porous, and very lightweight structure (Gizli *et al.* 2022), where the dispersed phase is air (Guastaferro *et al.* 2021). They can be either inorganic or organic in origin. Organic aerogels can be prepared from biologically based polymers, such as proteins and polysaccharides (Nita *et al.* 2020). In response to the growing demand for environmentally friendly alternatives, bio-based and bio-inspired aerogels have garnered significant interest due to their biocompatibility, potential biodegradability, and utilization of renewable raw materials. These characteristics are considered essential for biomedical and environmental applications (Guastaferro *et al.* 2021).

The preparation of various aerogels from renewable resources, such as starches, vegetable oils, and sugar cane, is well-documented in the literature, particularly for biomedical applications, including drug delivery systems (Nita *et al.* 2020; Karamikamkar

et al. 2023). This interest stems from their high porosity, large internal surface area, and cytological compatibility (Nita *et al.* 2020).

Starch is a renewable and biodegradable polysaccharide, the uses of which have attracted great interest in creating aerogels due to the material's ready availability, low cost, and versatility (Arvanitoyannis and Kassaveti 2009). Extracting starch from potato peel waste, a common agro-industrial by-product, offers a promising strategy for waste valorization and supports circular economy practices (Raigond *et al.* 2020; Barampouti *et al.* 2023). Native starch exhibits certain limitations, including brittleness, high water solubility, and limited mechanical strength, which collectively hinder its performance in specific applications. To address these challenges and expand the application potential of starch, chemical modifications—particularly cross-linking—have been employed to enhance its properties (Gonenc and Us 2019).

Native potato starch consists of amylose (mostly linear) and amylopectin (highly branched; not crosslinked). In cold water, starch granules are insoluble due to hydrogen bonding and semicrystalline packing; above the gelatinization temperature the granule swells, crystalline order is disrupted, amylose can leach and amylopectin becomes readily dispersible/soluble. Because these associations are physical rather than covalent, chemical crosslinking is sometimes applied after gelatinization when there is a reason to build a covalent network and tune swelling and release (Tester *et al.* 2004; Amaraweera *et al.* 2021).

Crosslinking introduces covalent bonds between starch chains, resulting in a three-dimensional network that improves the material's mechanical strength and its thermal stability. This modification also reduces the hydrophilic nature of starch, thereby decreasing its water solubility and enhancing its resistance to moisture. Such enhancements make crosslinked starch more suitable for applications requiring durability and stability under varying environmental conditions. Glutaraldehyde (Glu), a fixative agent used in biological research, is a widely employed crosslinking agent that can stabilize the starch network by forming covalent bonds between polymer chains prior to aerogel formation (Gadhave *et al.* 2019; Bassi *et al.* 2024).

By forming covalent bonds between the aldehyde groups of glutaraldehyde and the hydroxyl groups of starch, the mechanical properties and thermal stability of the resulting aerogel are improved, and its resistance to water-induced degradation is increased (Liang *et al.* 2016; Gonenc and Us 2019). This chemical modification results in a denser and more rigid network that is crucial for applications requiring durability and controlled release properties (Gadhave *et al.* 2019). However, glutaraldehyde's inherent toxicity poses challenges for specific applications, necessitating strategies to neutralize free residual glutaraldehyde to ensure the material's safety (National Center for Biotechnology Information 2025).

Glycine (Gly) is an amino acid and an important agricultural biostimulant to promote plant growth and health (Market Research Intellect 2025). Moreover, it can act as a neutralizing agent for residual glutaraldehyde by reacting through its amino groups with the aldehyde groups to form imine groups (Schiff bases) (Matei *et al.* 2020), resulting in a non-toxic product (Cheung and Brown 1982). Glycine's dual functionality can thus enhance the aerogel's suitability for agricultural applications, while mitigating potential safety concerns associated with glutaraldehyde toxicity, thereby expanding its scope of use in various fields (Cheung and Brown 1982; Market Research Intellect 2025).

This study examined the preparation and characterization of bio-based aerogels synthesized from cross-linked starch using varying concentrations of glutaraldehyde.

Incorporating glycine serves a dual purpose: both as a nutrient and a neutralizing agent for residual glutaraldehyde. The aerogels' structural, thermal, and functional properties were assessed to evaluate their potential for controlled glycine release and applications in sustainable agriculture.

EXPERIMENTAL

Materials

Potato peels from white potatoes (*Solanum tuberosum* L; cultivar not specified) were obtained as kitchen waste from a local restaurant in Quebec City (Canada); peels from a single collection day were pooled. Glutaraldehyde solution ($CHO(CH_2)_3CHO$; 50% wt in water), glycine (NH_2CH_2COOH; > 99.0% purity), ninhydrin ($C_9H_6O_4$; ≥99% purity), and perchloric acid ($HClO_4$; 70% solution in water) were purchased from MilliporeSigma (Oakville, ON, Canada). Phenol (C_6H_6O; ≥99% purity; stabilized) was purchased from Thermo Scientific (Ottawa, ON, Canada). Ethanol (C_2H_6O; 95% v/v) was pourchased from Commercial Alcohols (Brampton, ON, Canada). Sodium acetate anhydrous (CH_3COONa; ≥99% purity) was pourchased from Fisher Scientific (Ottawa, ON, Canada), and acetic acid (glacial) (CH_3COOH; ≥ 99.7% purity) was pourchased from Anachemia (Montréal, QC, Canada).

Starch Extraction from Potato Peels

Potato peels from white potatoes were washed, crushed with a blender, and filtered through a strainer. The potato peel filtrate was allowed to stand for 2 h, decanted, and then washed three or four times with deionized water (10 $mL.g^{-1}$ of starch per wash). The starch obtained after filtration was dried for 2 h at 50 °C and then stored in a plastic cup in a desiccator containing silica gel until use (Dorantes-Fuertes *et al.* 2024).

Synthesis of the Aerogels using Potato Peel Starch

The method used to prepare the aerogels was adapted from Liang *et al.* (2016), with adjustments in reagent volumes and microwave treatment time that were selected to ensure adequate gel formation. The protocol is illustrated in Fig. 1.

Ten grams of starch that was extracted from potato peels were weighed and added to 100 mL of deionized water. The mixture was agitated and heated to 80 °C for approximately 10 minutes until gelatinization occurred. The glutaraldehyde solution (0.2 to 1.0 mL of the 50% w/v commercial solution; Table 1) was then added, and the reaction mixture was microwaved at 800 W for 60 s (Liang *et al.* 2016), followed by washing with deionized water two or three times (10 $mL.g^{-1}$ of starch per wash). The hydrogel obtained was then immersed in 100 mL of a 0.3 M glycine solution (2.25 g/100 mL of deionized water) for 12 h at room temperature and again washed two or three times with deionized water (10 $mL.g^{-1}$ of starch per wash). It was then placed in a freezer (-80 °C) and lyophilized using a Labconco FreeZone ® freeze dryer (Labconco Corporation, Kansas, MO, USA) for 48 h under vacuum (≤ 0.133 mbar) with a condenser temperature of -85 °C to obtain an aerogel. Formulations were prepared on a 10 g dry-starch basis (Table 1) and all subsequent processing steps and reagent dosages were normalized to the mass of dry isolated starch (per g of starch).

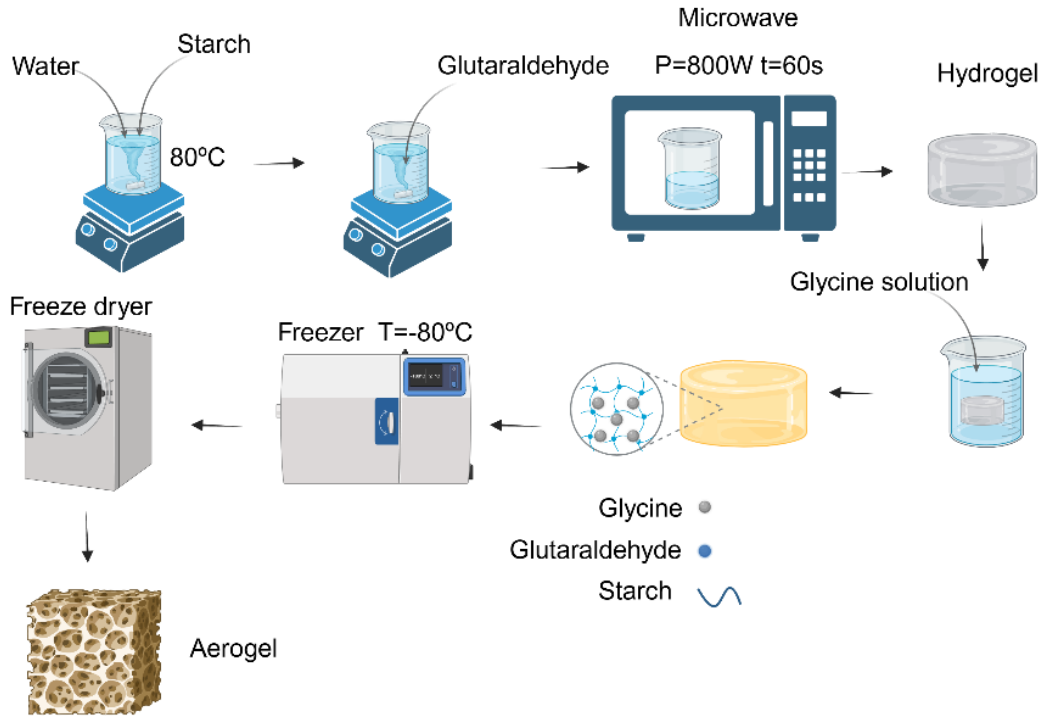

Fig. 1. Preparation of starch-based aerogels for glycine storage, controlled release, and glutaraldehyde neutralization

Table 1. Formulation of the Starch-based Aerogels Crosslinked with Glutaraldehyde, Without and With Glycine (Gly) Addition

Without Glycine addition			With Glycine	
Sample	Starch (g)	Glu (mL)	Sample	Gly (g)
AS0	10	0.0	AS0-Gly	2.25
AS1		0.2	AS1-Gly	
AS2		0.5	AS2-Gly	
AS3		1.0	AS3-Gly	
AS0 to AS3 refer to starch-based aerogels prepared without glycine. AS0-Gly to AS3-Gly corresponds to the same formulations after glycine was added. Glu (mL) = volume of 50% (w/v) glutaraldehyde solution per 10 g batch; Gly (g) = total mass added to a 100 mL, 0.3 M glycine batch.				

Characterization

The characterization was performed on aerogels prepared from potato peel starch, including non-crosslinked and glutaraldehyde crosslinked samples. In a second step, glycine was added to all formulations to assess its role in neutralizing glutaraldehyde. The methods described below were used to assess structural, morphological, and functional properties of the aerogels, including glycine storage and release behavior.

Fourier transform infrared spectroscopy (FTIR)

To study the chemical composition of the different aerogels prepared, as well as the extent of crosslinking, Fourier transform infrared spectroscopy was performed using an Invenio R spectrometer (Bruker, Billerica, MA, USA) equipped with a Platinum Attenuated Total Reflectance (ATR) accessory (A225/Q). Spectra were recorded in the

4000 to 400 cm^{-1} range with a resolution of 4 cm^{-1}, and a number of scans of 32. Data processing was carried out using OPUS software (Bruker, Billerica, MA, USA). Spectra were baseline-corrected and min–max normalized (0-1) using the 1200 to 900 cm^{-1} region prior to comparison; quantitative comparaisons used band–intensity ratios relative to the 1020 cm^{-1} band. For each sample, spectra from three ATR contact spots were acquired and averaged.

Thermogravimetric analysis (TGA) and derivative thermogravimetric (DTG) analysis

The thermal degradation of aerogels with varying percentages of crosslinking agent was studied using thermogravimetric analysis (TGA 851e, Mettler Toledo). Samples were heated from 35 to 800 °C at 10 °C/min in a nitrogen atmosphere. The derivative thermogravimetry (DTG) curves were plotted to identify the temperature at which the maximum weight loss rate occurred, providing insights into the thermal stability of the samples.

Morphology of glycine-loaded starch-based aerogels

The aerogel's porous morphology was examined using scanning electron microscopy (SEM) with an FEI Inspect F50 microscope, operated at accelerating voltages of 5 and 15 kV. Before the observation, the aerogels were coated with a 20 nm thick Pt/Pd layer using the sputter coater AGB7234 - Dry (Agar Scientific, Parsonage, England). Pore size measurements were performed using the XTMicroscope control integrated into SEM system. A total of 50 pores were measured per sample across different representative regions to ensure statistical significance, following the practices reported in the literature for pore analysis in porous biomaterials (Jayawardena *et al.* 2023).

Swelling degree (SD)

The degree of swelling of starch aerogels crosslinked with different concentrations of glutaraldehyde was determined using the method described by Durpekova *et al.* (2021). Dried aerogels (500 mg) were immersed in 25 mL of distilled water, and water absorption (WA) was monitored gravimetrically at 30 min and subsequently at 1, 2, 4, 6, 8, 12, 16, and 24 h using Eq. 1,

$$SD\ (\%) = \frac{m_f - m_i}{m_i} \times 100\% \quad (1)$$

where m_f is the weight of the wetted structure and m_i is the weight of the structure prior to water immersion (Tomadoni *et al.* 2019). Three replicate determinations were conducted for each aerogel.

Determination of residual glutaraldehyde

The protocol used to determine the amount of residual glutaraldehyde in the solution was adapted from previous work (Boratynski and Zal 1990; Gonenc and Us 2019). Before adding the glycine solution, the hydrogels were immersed in 100 mL of water for 24 h to allow the diffusion of unreacted glutaraldehyde. From this solution, a 0.5 mL aliquot was taken and mixed with the reagent, prepared by adding 40 µL of a 5% phenol solution to 10 mL of 70% perchloric acid. The mixture was dark incubated for 30 min. Under these acidic conditions, glutaraldehyde reacts with phenol to form a yellow-coloured complex. The intensity of this yellow colour, which was measured by absorbance at 480 nm using a double-beam UV-Vis spectrophotometer (Agilent Cary 60 UV-Vis), is directly

proportional to the concentration of free glutaraldehyde in the sample. The concentration was determined using a calibration curve (see supplementary information) (Boratynski and Zal, 1990). Three replicate determinations were conducted for each aerogel.

Glycine release study (GRS)

Distilled water was used as the release medium to measure the glycine concentration released from the aerogels. An aerogel was placed in an Erlenmeyer flask with 100 mL of the release medium (distilled water). At predetermined time intervals (2, 4, 6, 12, 24, 48, 72, 96 and 120 h), a 1 mL aliquot of the liquid phase was withdrawn. After each sampling, 1 mL of fresh release medium was added to maintain a constant total volume throughout the experiment. The collected volume (1 mL) was reacted with the ninhydrin reagent; the absorbance was measured at 570 nm, and the glycine concentration was calculated using the calibration curve (supplementary information) (Sun *et al.* 2006). Equation 2 was used to calculate the glycine release percentage (Sarhan *et al*. 2024).

$$Release\ (\%) = \frac{Concentration\ of\ released\ Glycine}{Glycine\ concentration\ in\ the\ aerogel} \times 100\% \quad (2)$$

For this analysis, three replicate determinations were conducted for each aerogel.

RESULTS AND DISCUSSION

The synthesis of starch-based aerogels involved chemical transformations that contributed to the material's structural and functional properties. Starch was crosslinked with glutaraldehyde through microwave-assisted heating, resulting in the formation of covalent bonds between polymer chains. Glycine was subsequently added to react with residual aldehyde groups, leading to the formation of imine linkages (Schiff bases) at pH 5 to 7. These reactions are illustrated in Fig. 2. These chemical modifications directly affect the material's molecular structure and properties, as the physicochemical and functional analyses that are described below demonstrate.

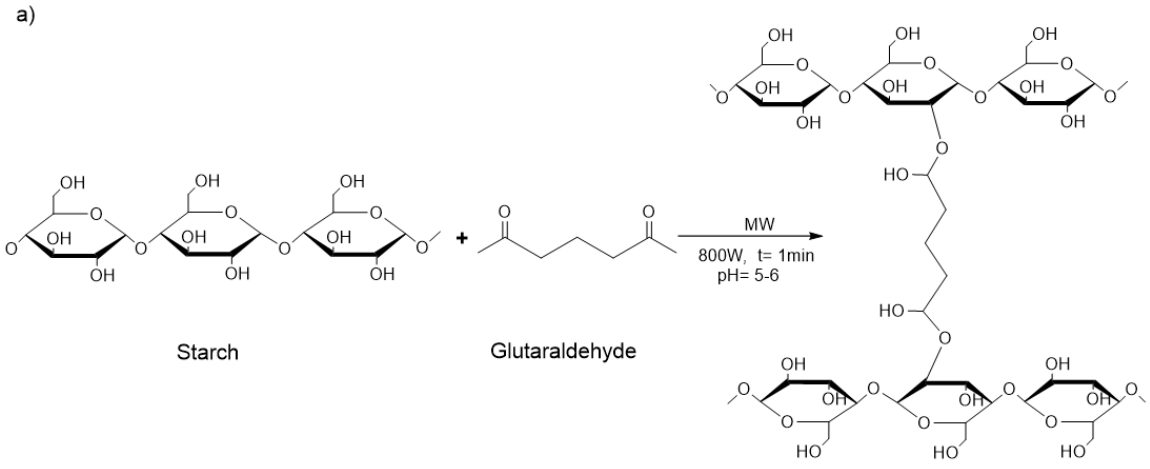

Fig. 2 (a). Proposed chemical reactions: (a) Crosslinking of starch with glutaraldehyde under microwave irradiation (800 W, 1 min); (b) Formation of Schiff base between glutaraldehyde and glycine at pH 5 to 7

b)

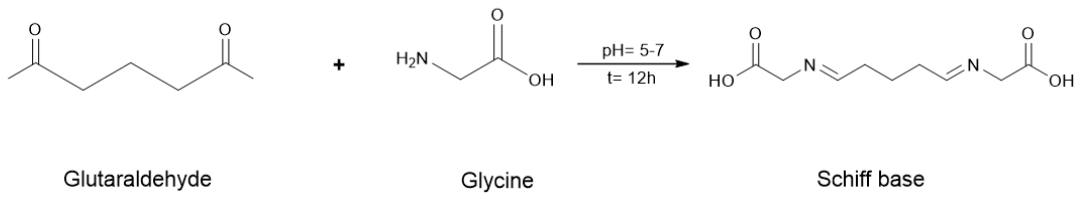

Fig. 2 (b). Proposed chemical reactions: (a) Crosslinking of starch with glutaraldehyde under microwave irradiation (800 W, 1 min); (b) Formation of Schiff base between glutaraldehyde and glycine at pH 5 to 7

Chemical Composition of the Aerogels

Figure 3 displays the FTIR spectra of the unmodified potato starch (AS0), as well as the crosslinked starch aerogels (AS1, AS2, AS3). The starch aerogel (AS0) spectrum presents the characteristic bands of starch that confirm its chemical structure: a peak at 3300 cm^{-1} that is associated with the stretching vibration of the -OH bonds, a peak at 2980 cm^{-1} corresponding to the asymmetric stretching vibration of the C-H bonds, the peaks at 1427 and 1363 cm^{-1} that are associated with the CH_2 scissoring and twisting vibrations, and the band in the range of 950 to 1150 cm^{-1}, which corresponds to the C-O-C vibrations (Camani *et al.* 2021).

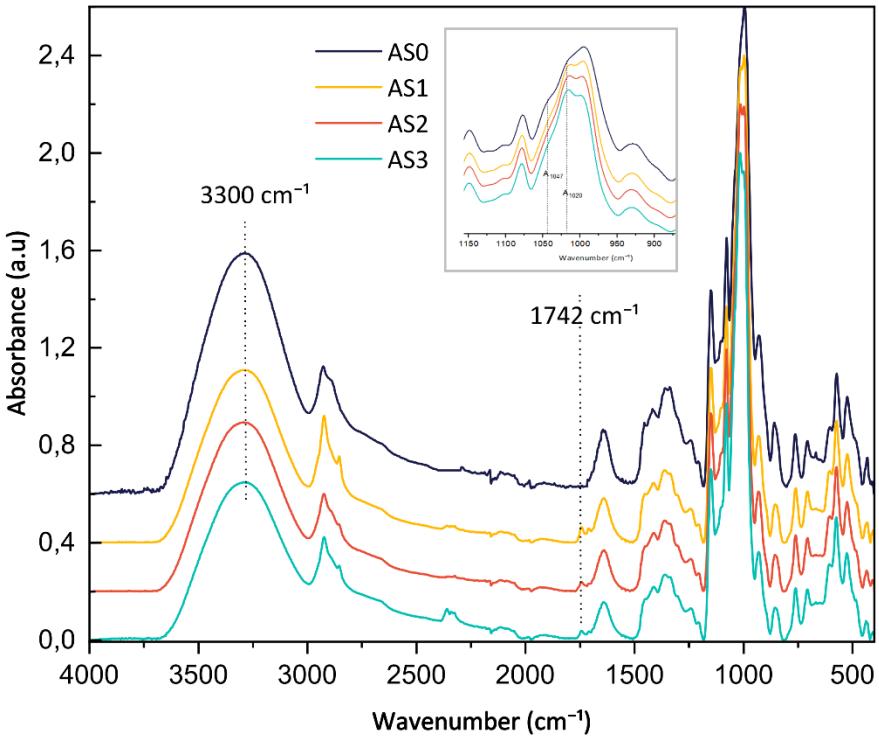

Fig. 3. FTIR spectra of the aerogels without glycine. AS0: non-crosslinked starch aerogels; AS1 – AS3: Starch aerogels crosslinked with increasing concentrations of the crosslinking agent. Spectra were baseline-corrected and normalized using the 1200-900 cm^{-1} region.

The spectrum of starch crosslinked with glutaraldehyde shows changes that are attributed to the formation of chemical bonds between the starch hydroxyl groups and glutaraldehyde. After normalization, the broad O-H stretching band (3300 cm^{-1}) shows a comparable profile across all samples. Quantitative comparisons are based on the short – range order index A_{1047}/A_{1020}, while other spectral changes are evaluated from band positions and the appearance/disappearance of characteristic features, consistent with modifications of the hydrogen-bonding network upon crosslinking. A new peak is observed at 1742 cm^{-1} for all crosslinked samples, which is attributed to C=O stretching vibrations of aldehyde groups, indicating the presence of unreacted glutaraldehyde in the modified matrices (Liang *et al.* 2016). At the lowest GA level tested (AS1), this ~1742 cm^{-1} band was detectable prior to glycine loading; GA doses below this were not investigated and may fall at or below the ATR-FTIR detection threshold.

A detailed comparison of the 950 to 1150 cm^{-1} region (Fig. 3) reveals a slight shift of the main absorption band toward higher wavenumbers in the crosslinked samples (AS1–AS3) compared to the non-crosslinked gelatinized starch (AS0). This region corresponds to C–O–C and C–C stretching vibrations in the polysaccharide structure of starch. These changes are attributed to structural rearrangements resulting from the progressive incorporation of glutaraldehyde into the starch network through crosslinking. Under the mildly acidic to near-neutral conditions that were used (pH 5 to 6), the reaction between aldehyde groups of glutaraldehyde and hydroxyl groups of starch leads to the formation of hemiacetal linkages, which influence the vibrational behavior of the C–O–C and C–C bonds. This effect is reflected in the observed spectral shift.

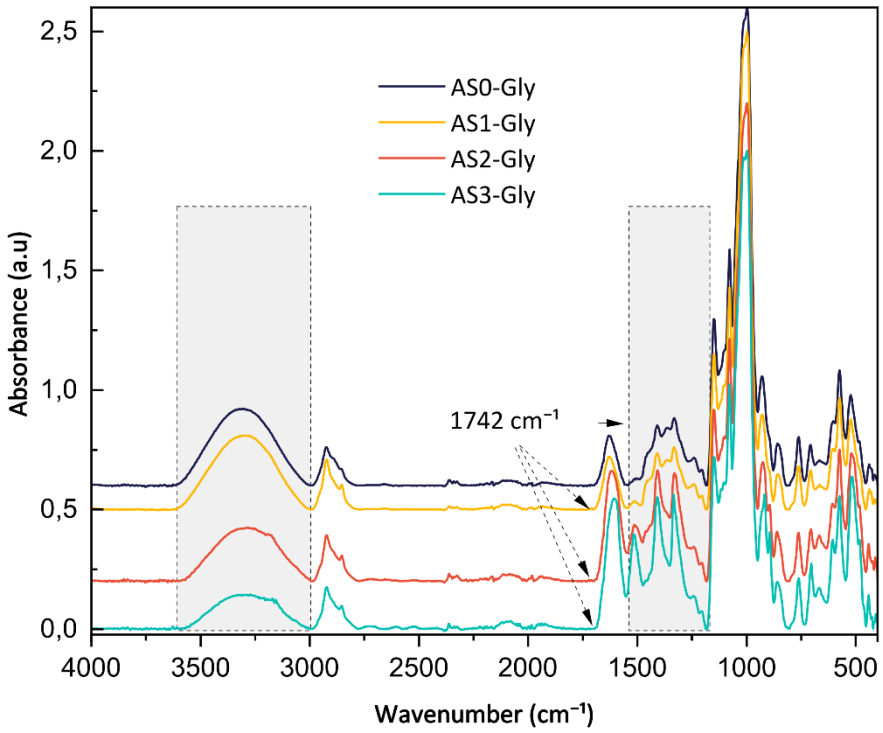

Fig. 4. FTIR spectra of the starch aerogels after glycine loading. AS0-Gly: non-crosslinked aerogel loaded with glycine; AS1-Gly to AS3-Gly: crosslinked aerogels loaded with glycine. Spectra were baseline-corrected and normalized using the 1200-900 cm^{-1} region.

Similar spectral changes have been reported by Lian *et al.* (2016) at pH 3 during microwave-assisted crosslinking of starch with glutaraldehyde. In both studies, increasing glutaraldehyde content led to a shift in the C–O–C band towards higher wavenumbers, indicating modifications in the molecular structure of the starch matrix. The decrease in the absorbance ratio A_{1047}/A_{1020}, from 0.71 in AS0 to 0.62 in AS3, suggests a reduction in the short-range molecular organization of starch, which is consistent with previous studies that have used this ratio to assess structural changes in starch during gelatinization and chemical modification (van Soest *et al.* 1995). When the crosslinked starch is loaded with glycine, additional modifications to the spectra are observed (Fig. 4).

The peak at 1742 cm^{-1}, corresponding to the aldehyde groups of the remaining glutaraldehyde, disappeared, indicating that glutaraldehyde had reacted with the amino groups ($-NH_2$) of glycine to form imine-like bonds (-C=N). This reaction resulted in a shift of the peak around 1610 cm^{-1}, confirming the formation of Schiff bases between glutaraldehyde and glycine (Kumar *et al.* 2021). In the 1550 to 1100 cm^{-1} region, bands became more prominent after normalization, consistent with N-H deformations and C-N stretching of glycine adsorbed on the aerogel (Rani *et al.* 2011). The O–H/N–H stretching band near 3300 cm^{-1} appeared less pronounced after glycine loading. At near-neutral pH, glycine is predominantly zwitterionic ($NH_3^+–CH_2–COO^-$) and therefore does not contribute a carboxylic O–H stretch; together with imine (Schiff) formation between residual aldehydes and primary amines, this reduces the population of free N–H and makes the broad O–H/N–H band near 3300 cm^{-1} appear less pronounced under normalized comparison (Max *et al.* 1998). The presence of glycine's functional groups (–NH and –COOH) and the formation of imines reorganize hydrogen-bonding interactions within the aerogel, which is reflected in the qualitative change of the ~3300 cm^{-1} profile. Similar behavior has been reported in chitosan-glutaraldehyde hydrogels, where the reaction between amines and aldehydes results in a decrease in the broad band around 3300 cm^{-1} due to the consumption of N-H groups and the reorganization of hydrogen bonds (Kumar *et al.* 2021).

Thermogravimetric and Derivative Thermogravimetric Analyses

TGA analysis of starch aerogels crosslinked with varying percentages of glutaraldehyde and loaded with glycine (Fig. 5) highlights the effect of crosslinking on thermal stability.

A minor weight loss below 100 °C was observed in all samples, which can be attributed to the evaporation of absorbed water, commonly associated with hydroxyl groups in starch (Liu *et al.* 2009). Between 200 and 260 °C, a more pronounced weight loss is observed, which can be attributed to the thermal degradation of glycine, as reported in previous studies (Weiss *et al.* 2018; Pokorný *et al.* 2024). This was confirmed by the thermal behavior depicted in Fig. 5. Notably, the AS3-Gly sample exhibited the highest weight loss in this region, indicating that a greater quantity of glycine remained trapped within the denser crosslinked network and subsequently underwent thermal degradation. In contrast, the AS0-Gly sample exhibited the lowest weight loss in this range, likely due to its more open-pore structure, which reduced its ability to retain glycine within the aerogel matrix. Finally, the thermal decomposition of all samples began within the range of 260 to 280 °C, as indicated by the onset temperatures in Fig. 5. The non-crosslinked aerogel (AS0-Gly) exhibited an initial degradation temperature of approximately 264±1.4 °C, corresponding to the onset of thermal degradation of the starch matrix (Ahmadzadeh *et al.* 2024). In comparison, the crosslinked samples exhibited a small but systematic shift

toward higher onset temperatures (AS1-Gly: 272 ± 1.1 °C, AS2-Gly: 275 ± 0.7 °C, AS3-Gly: 277 ± 1.0 °C), indicating that glutaraldehyde crosslinking enhanced the thermal stability of the starch network. This trend was further supported by an additional formulation prepared with 10% glutaraldehyde, which exhibited a higher onset degradation temperature of approximately 298 ± 1.2 °C (data not shown), consistent with the increased thermal resistance typically associated with higher glutaraldehyde content.

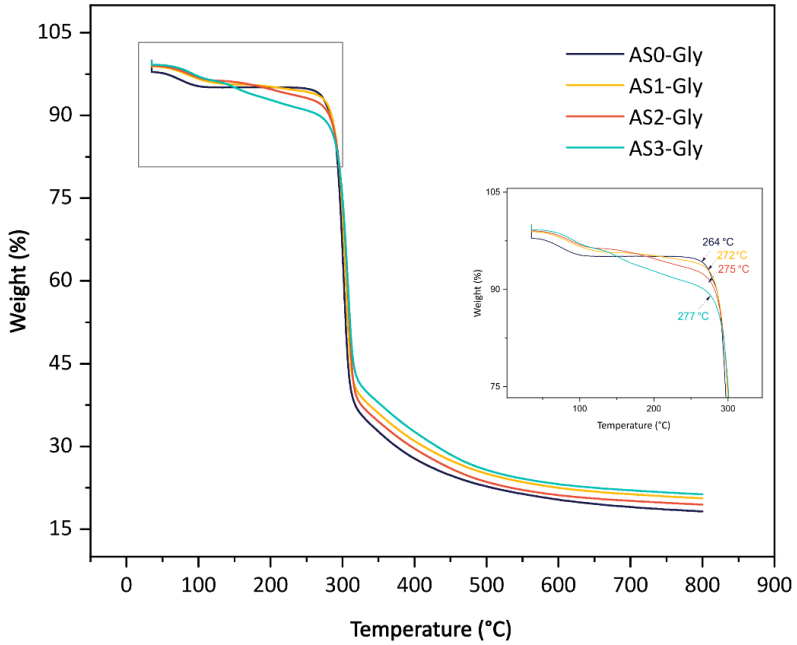

Fig. 5. Thermogravimetric analysis (TGA) curves of starch-based aerogels loaded with glycine (AS0-Gly to AS3-Gly)

The derivative thermogravimetric (DTG) curves (Fig. 6) provide additional insight into the aerogel's thermal behavior, showing a slight shift in the temperature of the maximum degradation rate from 302 °C (AS0-Gly) to 309 °C (AS3-Gly).

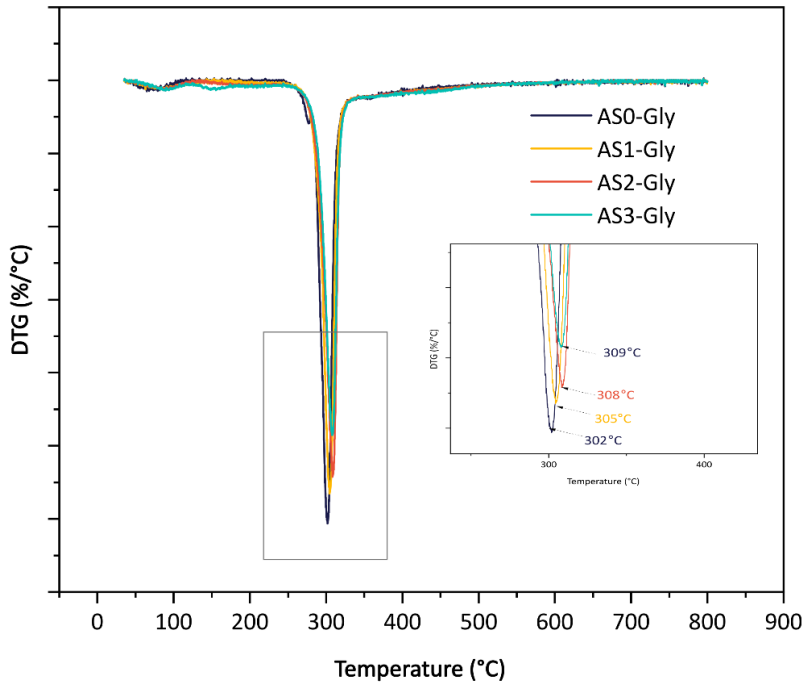

Fig. 6. Derivative thermogravimetric (DTG) curves of starch-based aerogels loaded with glycine

Crosslinking with glutaraldehyde enhances thermal stability, as evidenced by this shift. The covalent bonds formed between the aldehyde groups of glutaraldehyde and the hydroxyl groups of starch result in a more rigid and thermally stable network (Gadhave *et al.* 2019). Overall, the TGA and DTG results indicated small yet systematic improvements in thermal resistance of the aerogels, consistent with the formation of a denser network that restricts polymer mobility and increases the energy required for decomposition. While the difference in degradation onset temperature was relatively small, the effect of crosslinking was still apparent in AS3-Gly, which retained more glycine within the structure. This led to a more pronounced weight loss between 200 to 260 °C, which can be attributed to the thermal degradation of glycine.

Morphology of Glycine-Loaded Starch-Based Aerogels

The porous structure of aerogels loaded with glycine was observed using scanning electron microscopy (SEM), revealing that the non-crosslinked aerogel (AS0-Gly) (Fig. 7a) had a more irregular and collapsed structure. However, with increasing glutaraldehyde concentration, the aerogels exhibited an increasingly compact and homogeneous pore network.

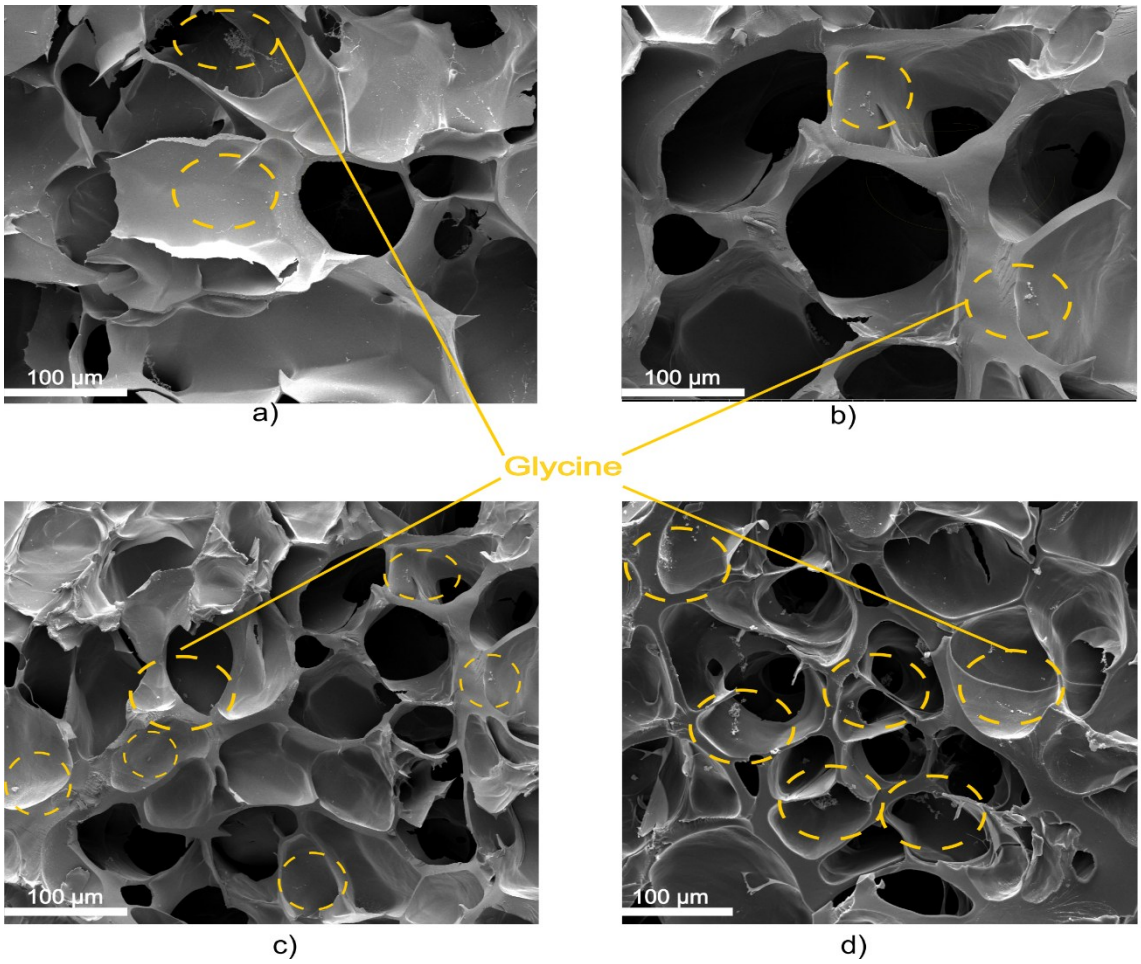

Fig. 7. SEM Images glycine crystals embedded in the porous structure of crosslinked starch aerogels: a) AS0-Gly, b) AS1-Gly, c) AS2-Gly, d) AS3- Gly. Scale bars: 100 µm. Labels "Glycine" and dashed circles indicate crystal-like deposits attributed to glycine (assignment supported by FTIR/TGA).

This visual change is attributed to the strengthening of the starch matrix by the hemiacetal bonds that are formed between the aldehyde group from Glu and the hydroxyl groups (starch) (Gonenc and Us 2019). Regarding glycine, SEM images revealed the presence of crystals distributed both on the surface and within the pores of the aerogel. Because SEM does not provide chemical specificity, these features were judged to be crystal-like deposits associated with glycine. This view is supported by complementary evidence: (i) FTIR after loading (disappearance of the ~1742 cm^{-1} aldehyde band and changes near ~1610 cm^{-1} and in the 1550–1100 cm^{-1} region), and (ii) TGA showing an additional weight-loss event at 200–260 °C assigned to glycine. This phenomenon was especially noticeable in the aerogel with higher concentrations of glutaraldehyde (AS2-Gly and AS3-Gly) (Figs. 7c and 7d), where a greater quantity of glycine crystals was observed being deposited in the aerogel cavities. In contrast, for the aerogels with lower crosslinker concentrations (AS1-Gly) (Fig. 7b) and without crosslinking (AS0-Gly) (Fig. 7a), the glycine crystals were more widely dispersed, most probably because the pores are larger and less defined, and the glycine was more broadly spread on the surface than inside the aerogel pores. This observation agrees with the pore size distribution analysis (Fig. 8),

which revealed a progressive reduction in pore size as the glutaraldehyde concentration increased.

The AS0-Gly exhibited the largest pores (62.1 ± 23.9 µm), followed by AS1-Gly (49.2 ± 16.7 µm), AS2-Gly (42.3 ± 10.5 µm), and AS3-Gly, which exhibited the smallest pores (20.5 ± 6.6 µm). These differences in pore size were statistically significant ($p < 0.05$), as confirmed by ANOVA followed by Tukey's post hoc test. Treatments that do not share the same letter in Fig. 8 (a, b, c) were significantly different from each other.

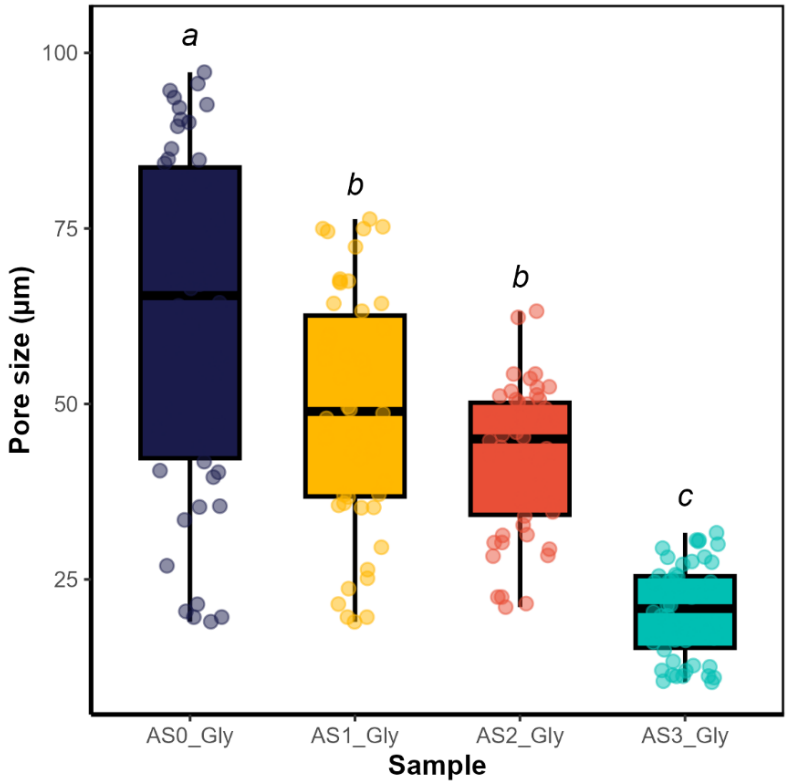

Fig. 8. Pore size distribution of glutaraldehyde-crosslinked starch aerogels loaded with glycine

This statistically significant trend supports the interpretation that crosslinking influences pore structure. These results indicate that as crosslinking increased, the aerogel network became more compact, resulting in a reduction of pore size and providing confined spaces for glycine deposition. In contrast, aerogels with lower crosslinking presented a more open structure with larger pores, allowing glycine to distribute more freely across the surface rather than being predominantly retained predominantly inside the pores. This trend is consistent with previous studies showing that increasing the concentration of the crosslinking agent leads to a more compact network and smaller pore sizes (Sringam *et al.* 2022; Mugnaini *et al.* 2023).

Swelling Degree (SD)

Figure 9 shows the swelling degree of aerogels that were loaded with glycine at various time intervals from t=0 (time zero) to t=24 h. The non-crosslinked aerogel (AS0-Gly) exhibited the greatest water absorption capacity, reaching nearly 1000% in the first h. This was attributed to the available hydroxyl groups (-OH) interacting with water molecules. However, due to the weakness of the hydrogen bond forces that bind the starch

macromolecules (amylose and amylopectin), as well as formation of hydrogen bonds between the starch chains and water molecules, the aerogel had almost completely dissolved after 6 h (Huang *et al*. 2023).

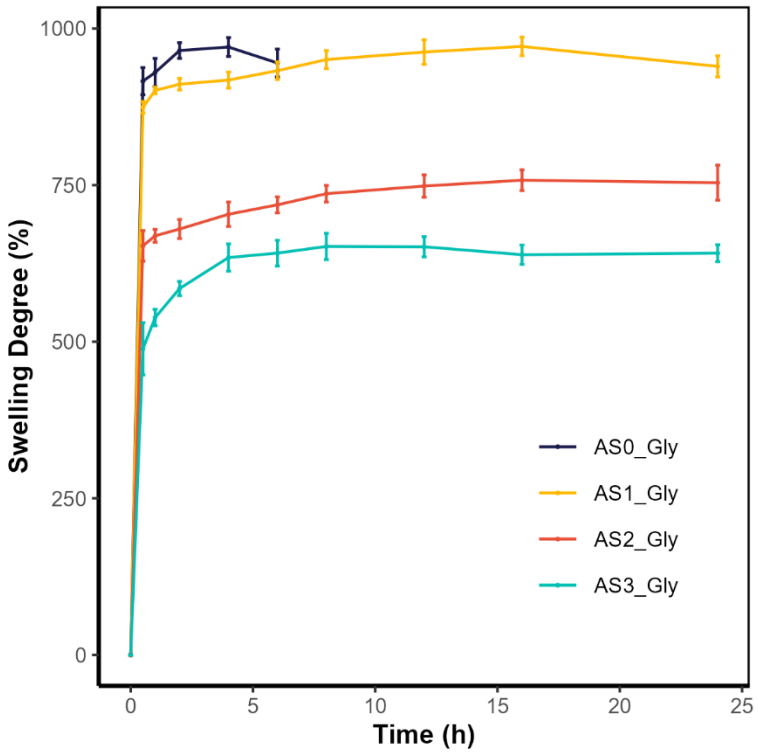

Fig. 9. Swelling degree of glutaraldehyde-crosslinked starch aerogels that were loaded with glycine as a function of time

The progressive decrease in water absorption observed with increasing crosslinker concentration can be attributed to the formation of a more compact and less flexible polymer network, which limits matrix expansion and reduces the amount of water retained. This behavior is consistent with previous studies, which report that highly crosslinked hydrogels restrict swelling and water uptake due to reduced free volume and the formation of hydrogen bonds with water molecules (Wu *et al.* 2009). This trend is also described by standards such as ASTM D2765, where swelling is used as an indirect indicator of crosslinking density (ASTM International 2020).

In the context of this study, the lower swelling that was observed in AS2 and AS3 suggests a denser network, which would be expected to affect the diffusion of encapsulated molecules. This relationship is explored further in the section dealing with glycine release.

Determination of Residual Glutaraldehyde

The quantification of residual glutaraldehyde (Residual Glu, mM) in the aerogels before glycine addition revealed a direct monotonic correlation between crosslinker concentration and unreacted aldehyde content (Fig. 10a). As the glutaraldehyde concentration was increased from AS1 to AS3, a progressive rise in residual aldehyde was observed, with AS3 showing the highest concentration (~1.5 mM). Glutaraldehyde was not detected in the non-crosslinked AS0 sample, as expected.

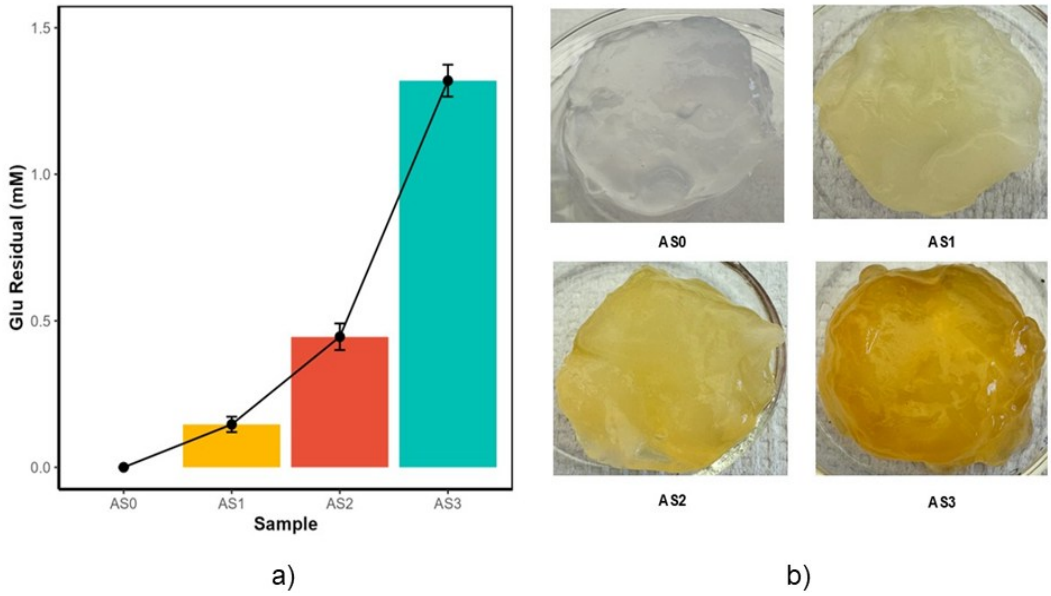

Fig. 10. (a) Residual glutaraldehyde concentration in each sample, and (b) Visual appearance of gels after glycine addition

This trend suggests that as the glutaraldehyde concentration was increased, the availability of reactive hydroxyl groups in the starch matrix may have become limiting, resulting in unreacted glutaraldehyde remaining in the gel. Yet, this may also have been influenced by the specific reaction conditions, which may have limited the extent of glutaraldehyde consumption. Crosslinking continued to increase across AS1 to AS3; however, no clear plateau was observed in crosslinking-related indicators. The accumulation of free aldehyde at higher concentrations may reflect this limitation in hydroxyl availability or reaction kinetics. In turn, this behavior suggests that the system could have been approaching the maximum crosslinking capacity under the tested conditions.

Additionally, the mildly acidic to near-neutral pH (5 to 6) used during gelation may also influence the reactivity and stability of hemiacetal linkages formed between aldehyde and hydroxyl groups. While hemiacetal formation is favored under these conditions, the formation of acetal linkages is unlikely to take place in aqueous media and would typically require stronger acid catalysis and water removal. Although these linkages are reversible in aqueous environments, the resulting network may remain stable under the preparation and intended application conditions, particularly when free aldehyde is subsequently neutralized.

To reduce the amount of unreacted glutaraldehyde, glycine was added to the hydrogel before it was freeze-dried (Sapuła *et al.* 2023). Glycine reacts with free aldehyde groups through Schiff base formation (Marquié 2001). This reaction can proceed under mildly acidic to neutral aqueous conditions (pH ~5 to 7) and at room temperature, where the amino group remains sufficiently nucleophilic to react with aldehyde functionalities (Cheung and Brown 1982). The formation of Schiff bases was visually observed as a yellow-to-orange coloration in the hydrogel (Fig. 10b). This coloration is attributed to the formation of Schiff bases between glycine and free aldehyde groups (Mugnaini *et al.* 2023). Although the presence of free reducing sugars was not confirmed in this system, and glycine was added only after the crosslinking and cooling steps, one cannot fully exclude

the occurrence of side reactions, most notably, the reaction between glutaraldehyde and glycine leads to the formation of a Schiff base, which is also a typical product of the initial step in Maillard type reactions (Laroque *et al.* 2008; Provost 2019). However, classical Maillard reactions typically require the presence of reducing sugars, elevated temperatures, and a more neutral to alkaline pH, none of which were present under the conditions that were used in this study (Provost 2019).

The progressive increase in color intensity with glutaraldehyde concentration (Ibarra 2022) is consistent with the greater availability of free aldehyde groups, further supporting the results obtained in the quantification assay.

These findings confirm that while increasing glutaraldehyde concentration enhanced network formation, it also led to the presence of residual aldehyde groups that were not fully consumed during crosslinking. This behavior highlights the importance of balancing crosslinker content with available reactive sites within the starch matrix. This balance likely depends not only on stoichiometric considerations (*e.g.*, OH/CHO ratio), but also on reaction parameters such as time and microwave power, which were selected based on preliminary observations and maintained constant throughout the experiments. In this work, the use of glycine after gelation effectively addressed this obstacle, enabling the neutralization of unreacted aldehydes and contributing to the biocompatibility of the final aerogels (Sapuła *et al.* 2023).

Glycine Release Study (GRS) and Kinetic Study of Glycine Release

The behavior of glycine release from four different starch aerogels, prepared with increasing glutaraldehyde concentrations, was examined in water at room temperature over a 120-h period (Fig. 11). The findings indicate that crosslinker concentration had a marked effect on glycine release. The non-crosslinked aerogel (AS0-Gly) exhibited a rapid and uncontrolled release due to the rapid loss of structural integrity upon hydration. Lacking a crosslinked polymeric network to maintain integrity, the aerogel progressively dissolved, releasing nearly all its glycine content within the first few h, thereby failing to sustain its release over time.

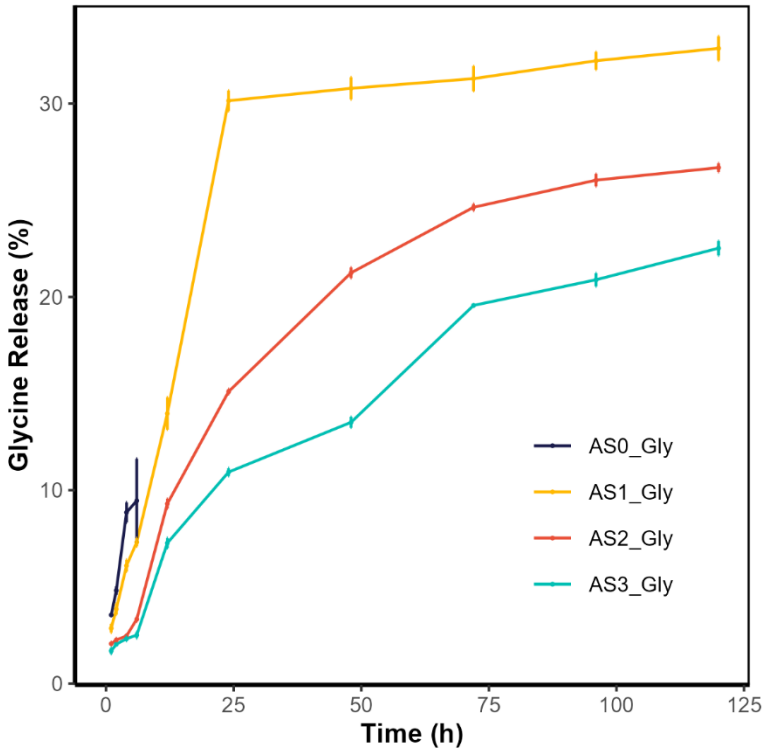

Fig. 11. Percentage of glycine that was released from glutaraldehyde-crosslinked starch aerogels as a function of time

In contrast, the crosslinked aerogels exhibited more controlled release profiles. The aerogel that was crosslinked with 0.2% glutaraldehyde (AS1-Gly exhibited the highest cumulative release among the crosslinked samples, reaching 65.5 ± 1.2% over 120 h. Formulations with 0.5% (AS2-Gly) and 1% glutaraldehyde (AS3-Gly) showed lower cumulative releases of 53.2 ± 0.4% and 44.9 ± 0.7%, respectively. This reduction is attributed to the increasing crosslinking density, which results in smaller pore sizes and a more compact network that hinders glycine diffusion (Fig. 8) (Sringam *et al.* 2022). The low standard deviations (SD) observed across replicates suggest good consistency between measurements, in line with previous reports on the release of drugs or nutrients from crosslinked biopolymer matrices (Abouelmagd *et al.* 2015; Sarhan *et al.* 2024).

The release profile showed a distinct two-stage release pattern. AS1-Gly released nearly 60% of its glycine within the first 10 h, which was likely due to surface-adsorbed glycine or loosely retained molecules within the matrix. AS2-Gly and AS3-Gly exhibited more gradual initial release stages, suggesting stronger interactions between glycine and the crosslinked polymeric network. This was followed by a slower and sustained release, especially in the more densely crosslinked aerogels, indicating that the remaining glycine was more tightly embedded within the matrix structure (Bassi *et al.* 2024).

The progressive decrease in glycine release with increasing glutaraldehyde concentration is consistent with the more compact polymeric networks that were observed in the analysis of swelling behavior (Fig. 9). Swelling capacity is widely used as an indirect indicator of crosslinking density in hydrogel and aerogel systems, given that tighter networks absorb less water and restrict molecular diffusion (Durpekova *et al.* 2021).

Kinetic Study of Glycine Release

The glycine release profiles from starch aerogels that were crosslinked with varying glutaraldehyde concentrations were analyzed using zero-order, first-order, Higuchi, and Korsmeyer-Peppas kinetic models. The zero-order model describes release as a continuous process with a constant rate, independent of the drug concentration in the matrix. In contrast, the first-order model assumes that the release rate is proportional to the amount of glycine remaining in the aerogel (Gouda *et al.* 2017). The Higuchi model, based on Fickian diffusion through a porous matrix, predicts a release rate proportional to the square root of time (Ramteke *et al.* 2014). Lastly, the Korsmeyer-Peppas model, meanwhile, accounts for both Fickian diffusion and potential relaxation or swelling of the polymer network and is particularly suitable for characterizing anomalous transport mechanisms (Zhu *et al.* 2023). Variations in the kinetic parameters among the samples are expected to reflect the influence of crosslinking density on diffusion and matrix structural dynamics.

Coefficients of determination (R^2) that were obtained from the fitting of each model to the experimental data are summarized in Table 2. The corresponding fitting curves are presented in Fig. 12. The AS0-Gly sample, which lacked a crosslinked network, exhibited the highest R^2 values across all models. This behavior reflects the uncontrolled release caused by rapid matrix disintegration upon hydration, rather than true diffusion-controlled kinetics. Although high R^2 values suggest a good fit to multiple models, they do not accurately represent a sustained or controlled release mechanism in the absence of a stable polymer network.

Table 2. Equations and Regression Coefficients of Kinetic Models for Glycine Release from Glutaraldehyde-crosslinked Starch Aerogels

Kinetics modal	Equations	Sample	R^2
Zero order	$C_t - C_0 = k_0 t$	AS0-Gly	0.9863
		AS1-Gly	0.7091
		AS2-Gly	0.8740
		AS3-Gly	0.9307
First order	$\ln C_0 - \ln C_t = k_1 t$	AS0-Gly	0.9809
		AS1-Gly	0.7125
		AS2-Gly	0.8276
		AS3-Gly	0.8855
Higuchi	$C_t = k_h t^{1/2}$	AS0-Gly	0.9428
		AS1-Gly	0.8128
		AS2-Gly	0.8699
		AS3-Gly	0.9363
Korsmeyer - Peppas	$M_t/M_\infty = k_p t^n$	AS0-Gly	0.9792
		AS1-Gly	0.9334
		AS2-Gly	0.9320
		AS3-Gly	0.9545

C_t and C_0 represent the glycine concentration at time *t* and the initial time, respectively. M_t/M_∞ corresponds to the fraction of glycine released at time *t*. The kinetic constants (k_0, k_1, k_h, k_p) and the exponent *n* in the Korsmeyer-Peppas model were fitted to the experimental data. The regression coefficient R^2 indicates how accurately each model fits the experimental data.

In contrast, the crosslinked aerogels (AS1-Gly, AS2-Gly, and AS3-Gly) demonstrated more sustained release profiles, with the best fits being observed for the Higuchi and Korsmeyer-Peppas models. The Higuchi model yielded R^2 values ranging from 0.8128 (AS1-Gly) to 0.9363 (AS3-Gly), indicating that glycine release was

predominantly governed by diffusion through the polymer matrix. Similarly, strong coefficients of determination ($R^2 \geq 0.9320$) were obtained with the Korsmeyer-Peppas model, suggesting that in addition to diffusion, matrix relaxation or swelling effects may also have contributed to the release behavior, particularly at lower crosslinking densities.

Among the crosslinked samples, AS3-Gly (highest glutaraldehyde concentration) consistently exhibited the best fit to the diffusion-controlled models, with R^2 values of 0.9363 (Higuchi) and 0.9545 (Korsmeyer-Peppas). This behavior is consistent with the observed decrease in swelling degree (Fig. 9) and pore size (Fig. 8) with increasing glutaraldehyde concentration, supporting the interpretation that higher crosslinking density leads to a denser polymeric network, reduced glycine diffusivity, and a more sustained release profile.

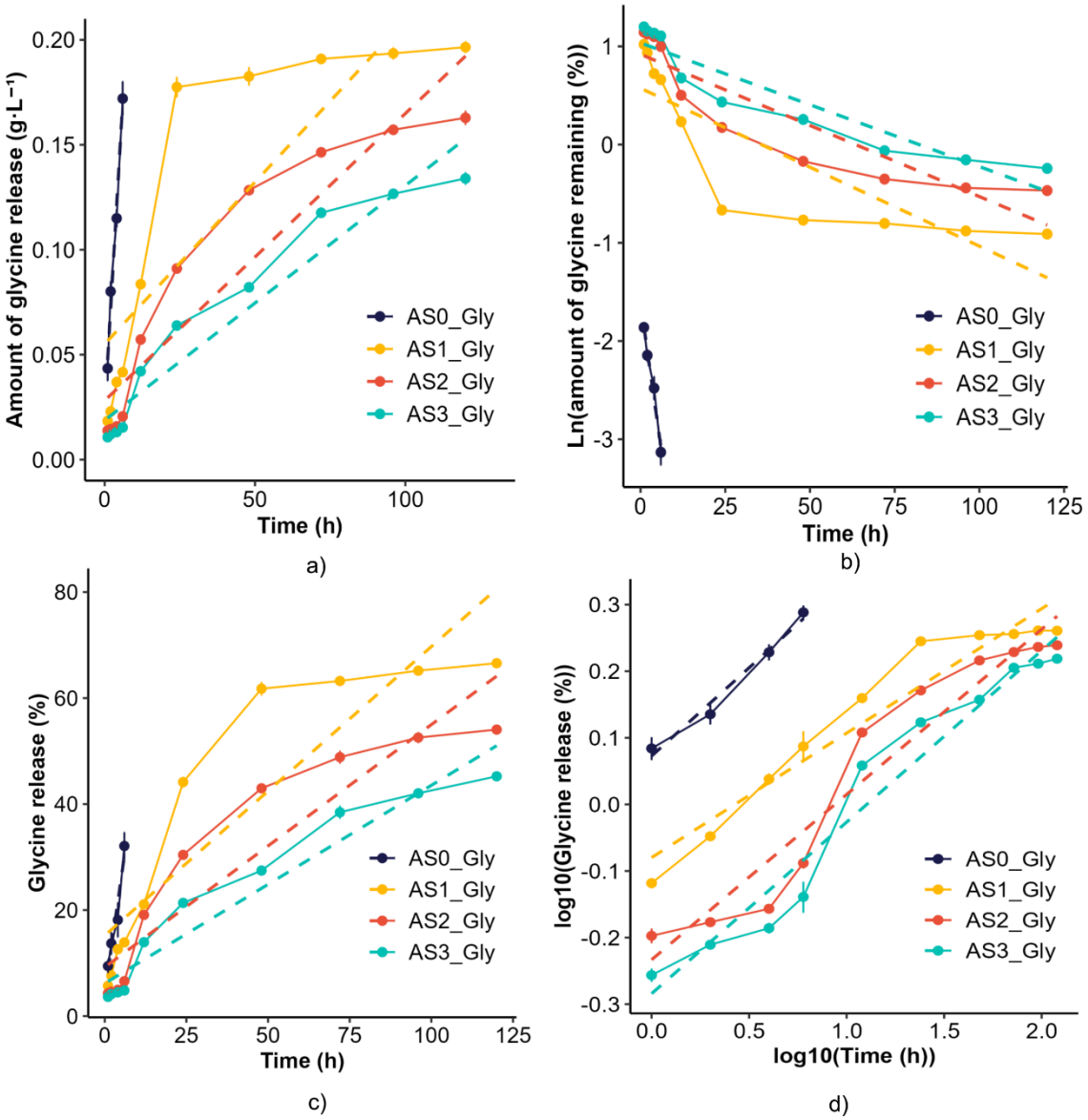

Fig. 12. Kinetic models of glycine release from glutaraldehyde-crosslinked starch aerogels: a) Zero order, b) First order, c) Higuchi, and d) Konsmeyer-Peppas. Solid lines represent experimental data; dashed lines indicate the best fit curves that were derived from the respective kinetic models.

These results are consistent with previous studies reporting that release from porous polymeric matrices often follows diffusion-controlled mechanisms. For instance, Zhu *et al.* (2023) observed that Higuchi and Korsmeyer best described drug release from viscose-based networks-Peppas models, consistent with the findings reported here. Similarly, Sarhan *et al.* (2024) demonstrated that increasing the network density in microalgae-based hydrogels led to slower fertilizer release, a phenomenon also associated with this study with higher crosslinking density and reduced swelling.

This study used white-potato peels from a single source. Because all steps were normalized per gram of dry isolated starch, the qualitative trends reported here (*e.g.*, the effect of glutaraldehyde crosslinking on water uptake and glycine release) are expected to apply for common table-potato cultivars, while absolute values may vary with cultivar.

CONCLUSIONS

1. This study aimed to develop and characterize bio-based aerogels from potato peel starch crosslinked with glutaraldehyde. It evaluated their potential as sustainable carriers for glycine storage and controlled release in agricultural applications. The findings demonstrated that crosslinking substantially enhanced the structural and thermal stability of the aerogels, as evidenced by Fourier transform infrared (FTIR) and thermogrametric (TGA) analyses. FTIR confirmed the successful formation of covalent bonds between glutaraldehyde and the hydroxyl groups of starch, while TGA revealed improved thermal stability in the cross-linked samples, with increased decomposition temperatures and a higher residual mass at high temperatures. Quantitatively, the short-range order index A_{1047}/A_{1020} decreased from 0.71 (AS0) to 0.62 (AS3), the ~1742 cm^{-1} aldehyde band disappeared after glycine loading, and the TGA onset temperature increased slightly from 264 ± 1.4 °C (AS0-Gly) to 277 ± 1.0 °C (AS3-Gly) with a slight DTG peak shift from 302 °C to 309 °C.
2. Morphological characterization by scanning electron microscope (SEM) highlighted that AS3-Gly exhibited the densest aerogel network, reducing pore size and influencing the distribution of glycine crystals within the matrix. These structural modifications directly affected the glycine release profile, given that AS1-Gly resulted in higher glycine release (~70% over 120 h), while AS2-Gly and AS3-Gly led to a more sustained and controlled release, following the Higuchi and Korsmeyer-Peppas diffusion models. Consistently, the mean pore size decreased from 62.1 ± 23.9 µm (AS0-Gly) to 49.2 ± 16.7 µm (AS1-Gly), 42.3 ± 10.5 µm (AS2-Gly), and 20.5 ± 6.6 µm (AS3-Gly) (ANOVA/Tukey, $p < 0.05$).
3. The incorporation of glycine also enabled its controlled release and played a key role in neutralizing residual glutaraldehyde, thereby mitigating potential toxicity towards biological systems, particularly in the context of seed germination. This neutralization process was confirmed by FTIR analysis (loss of the ~1742 cm^{-1} aldehyde band and changes near ~1610 cm^{-1} after glycine loading).
4. These results confirmed that starch-based aerogels derived from agricultural waste represent a viable and sustainable approach for developing eco-friendly controlled-release systems. Their capacity to effectively store and gradually release bioactive molecules, combined with their biodegradability and renewable origin, positions them as promising materials for agricultural applications and related sectors.

ACKNOWLEDGMENTS

The authors thank Yves Bédard, Nicola Larouche, and Flore Jezequel for their help. This work was supported by Sentinel North Canada First Research Excellence Fund for GENOSCAN project (Ecogenomics of mining areas for sustainable Canadian North).

REFERENCES CITED

Abouelmagd, S. A., Sun, B., Chang, A. C., Ku, J. Y., and Yeo, Y. (2015). "Release kinetics study of poorly water-soluble drugs from nanoparticles: Are we doing it right?" *Mol. Pharm.* 12(3), 997-1003. https://doi.org/10.1021/mp500817h

Ahmadzadeh, S., Sagardui, A., Huitink, D., Chen, J., and Ubeyitogullari, A. (2024). "Cellulose-starch composite aerogels as thermal superinsulating materials," *ACS Omega* 9, 49205-49213. https://doi.org/10.1021/acsomega.4c05840

Amaraweera, S. M., Gunathilake, C., Gunawardene, O. H. P., Fernando, N. M. L., Wanninayaka, D. B., Dassanayake, R. S., Rajapaksha, S. M., Manamperi, A., Fernando, C. A. N., Kulatunga, A. K., and Manipura, A. (2021). "Development of starch-based materials using current modification techniques and their applications: A review," *Molecules* 26(22), article 6880. https://doi.org/10.3390/molecules26226880

Arvanitoyannis, I. S., and Kassaveti, A. (2009). "Starch-cellulose blends," in: *Biodegradable Polymer Blends and Composites from Renewable Resources*, John Wiley & Sons, Hoboken, NJ, USA, pp. 17-53. https://doi.org/10.1002/9780470391501.ch2

ASTM D2765-01 (2020). "Standard test methods for determination of gel content and swell ratio of crosslinked ethylene plastics," ASTM International, West Conshohocken, PA, USA.

Barampouti, E. M., Christofi, A., Malamis, D., and Mai, S. (2023). "A sustainable approach to valorize potato peel waste towards biofuel production," *Biomass Convers. Biorefin.* 13(9), 8197-8208. https://doi.org/10.1007/s13399-021-01811-4

Bassi, M., Kalpana, R., and Kumar, V. (2024). "Starch glutaraldehyde cross linked hydrogel for drug release properties," *J. Pharm. Bioallied Sci.* 16(Suppl 2), S1198-S1200. https://doi.org/10.4103/jpbs.jpbs_538_23

Boratynski, J., and Zal, T. (1990). "Colorimetric micromethods for glutaraldehyde determination by means of phenol and sulfuric acid or phenol and perchloric acid," *Anal. Biochem.* 184, 259-262.

Camani, P. H., Gonçalo, M. G. M., Barbosa, R. F. S., and Rosa, D. S. (2021). "Comprehensive insight of crosslinking agent concentration influence on starch-based aerogels porous structure," *J. Appl. Polym. Sci.* 138(34). https://doi.org/10.1002/app.50863

Cheung, H. Y., and Brown, M. R. W. (1982). "Evaluation of glycine as an inactivator of glutaraldehyde," *J. Pharm. Pharmacol.* 34(4), 211-214. https://doi.org/10.1111/j.2042-7158.1982.tb04230.x

Dorantes-Fuertes, M. G., López-Méndez, M. C., Martínez-Castellanos, G., Meléndez-Armenta, R. Á., and Jiménez-Martínez, H. E. (2024). "Starch extraction methods in tubers and roots: A systematic review," *Agronomy* 14(4), article 865. https://doi.org/10.3390/agronomy14040865

Durpekova, S., Di Martino, A., Dusankova, M., Drohsler, P., and Sedlarik, V. (2021). "Biopolymer hydrogel based on acid whey and cellulose derivatives for enhancement water retention capacity of soil and slow release of fertilizers," *Polymers (Basel)* 13(19), article 3274. https://doi.org/10.3390/polym13193274

Gadhave, R. V., Mahanwar, P. A., and Gadekar, P. T. (2019). "Effect of glutaraldehyde on thermal and mechanical properties of starch and polyvinyl alcohol blends," *Des. Monomers Polym.* 22(1), 164-170. https://doi.org/10.1080/15685551.2019.1678222

Gizli, N., Çok, S. S., and Koç, F. (2022). "Aerogel, xerogel, and cryogel – Synthesis, surface chemistry, and properties," in: *Advanced Materials for Sustainable Environmental Remediation*, Elsevier, Amsterdam, pp. 195-229. https://doi.org/10.1016/B978-0-323-90485-8.00021-7

Gonenc, I., and Us, F. (2019). "Effect of glutaraldehyde crosslinking on degree of substitution, thermal, structural, and physicochemical properties of corn starch," *Starch/Stärke* 71(3–4). https://doi.org/10.1002/star.201800046

Gouda, R., Baishya, H., and Qing, Z. (2017). "Application of mathematical models in drug release kinetics of Carbidopa and Levodopa ER tablets," *J. Dev. Drugs* 6(2). https://doi.org/10.4172/2329-6631.1000171

Guastaferro, M., Reverchon, E., and Baldino, L. (2021). "Polysaccharide-based aerogel production for biomedical applications: A comparative review," *Materials* 14(7), article 1631. https://doi.org/10.3390/ma14071631

Huang, J., Gao, J., Qi, L., Gao, Q., and Fan, L. (2023). "Preparation and properties of starch-cellulose composite aerogel," *Polymers (Basel)* 15(21), article 4294. https://doi.org/10.3390/polym15214294

Ibarra, S. A. M. (2022). *Apósitos Citocompatibles de Quitosano-Gelatina para Aplicaciones Biomédicas*, Master's Thesis, Instituto Tecnológico de Tijuana, Baja California, Mexico.

Jayawardena, I., Turunen, P., Garms, B. C., Rowan, A., Corrie, S., and Grøndahl, L. (2023). "Evaluation of techniques used for visualisation of hydrogel morphology and determination of pore size distributions," *Mater. Adv.* 4(2), 669-682. https://doi.org/10.1039/d2ma00932c

Karamikamkar, S., Yalcintas, E. P., Haghniaz, R., de Barros, N. R., Mcewan, M., Nasiri, R., Davoodi, E., Nasrollahi, F., Erdem, A., Kang, H., Lee, J., Zhu, Y., Ahadian, S., Jucaud, V., Maleki, H., Dokmeci, M. R., Kim, H.-J., and Khademhosseini, A. (2023). "Aerogel-based biomaterials for biomedical applications: From fabrication methods to disease-targeting applications," *Adv. Sci.* 10(25), article 2204681. https://doi.org/10.1002/advs.202204681

Kumar, P., Pillay, V., and Choonara, Y. E. (2021). "Macroporous chitosan/methoxypoly (ethylene glycol)-based cryosponges with unique morphology for tissue engineering applications," *Sci. Rep.* 11(1), article 3104. https://doi.org/10.1038/s41598-021-82484-x

Laroque, D., Inisan, C., Berger, C., Vouland, É., Dufossé, L., and Guérard, F. (2008). "Kinetic study on the Maillard reaction: Consideration of sugar reactivity," *Food Chem.* 111(4), 1032-1042. https://doi.org/10.1016/j.foodchem.2008.05.033

Liang, W., Sanchez-Soto, M., Abt, T., Maspoch, M.L., and Santana, O. (2016). "Microwave-crosslinked bio-based starch-clay aerogels," *Polym. Int.* 65(8), 899-904. https://doi.org/10.1002/pi.5104

Liu, H., Xie, F., Yu, L., Chen, L., and Li, L. (2009). "Thermal processing of starch-based polymers," *Prog. Polym. Sci.* 34(12), 1348-1368.

https://doi.org/10.1016/j.progpolymsci.2009.07.001
Market Research Intellect. "Glycine market booms: Applications in health, food, and manufacturing propel growth," (https://www.marketresearchintellect.com/blog/glycine-market-booms-applications-in-health-food-and-manufacturing-propel-growth/), Accessed March 2, 2025.
Marquié, C. (2001). "Chemical reactions in cottonseed protein crosslinking by formaldehyde, glutaraldehyde, and glyoxal for the formation of protein films with enhanced mechanical properties," *J. Agric. Food Chem.* 49(10), 4676-4681. https://doi.org/10.1021/jf0101152
Matei, A., Puscas, C., Patrascu, I., Lehene, M., Ziebro, J., Scurtu, F., Baia, M., Porumb, D., Totos, R., and Silaghi-Dumitrescu, R. (2020). "Stability of glutaraldehyde in biocide compositions," *Int. J. Mol. Sci.* 21(9), article 3372. https://doi.org/10.3390/ijms21093372
Max, J.-J., Trudel, M., and Chapados, C. (1998). "Infrared titration of aqueous glycine," *Applied Spectroscopy* 52(2), 226-233. DOI: 10.1366/0003702981943284
Mugnaini, G., Gelli, R., Mori, L., and Bonini, M. (2023). "How to crosslink gelatin: The effect of glutaraldehyde and glyceraldehyde on the hydrogel properties," *ACS Appl. Polym. Mater.* 5(11), 9192-9202. https://doi.org/10.1021/acsapm.3c01676
National Center for Biotechnology Information (NCBI). "Health effects – Toxicological profile for glutaraldehyde," (https://www.ncbi.nlm.nih.gov/books/NBK591675/), Accessed March 2, 2025.
Nita, L. E., Ghilan, A., Rusu, A. G., Neamtu, I., and Chiriac, A. P. (2020). "New trends in bio-based aerogels," *Pharmaceutics* 12(5), article 449. https://doi.org/10.3390/pharmaceutics12050449
Pokorný, V., Štejfa, V., Havlín, J., Fulem, M., and Růžička, K. (2024). "Heat capacities of α-, β-, and γ-polymorphs of glycine," *Molecules* 29(22). https://doi.org/10.3390/molecules29225366
Provost, J. J. (2019). "The Maillard reaction," in: *Food Aroma Evolution: During Food Processing, Cooking, and Aging*, M. Bordiga and L. M. L. Nollet (eds.), CRC Press, Boca Raton, FL, pp. 1-11.
Raigond, P., Singh, B., Dutt, S., and Chakrabarti, S. K. (2020). *Potato: Nutrition and Food Security*, Springer, Singapore. https://doi.org/10.1007/978-981-15-7662-1
Ramteke, K. H., Dighe, P. A., Kharat, A. R., and Patil, S. V. (2014). "Mathematical models of drug dissolution: A review," *Scholars Acad. J. Pharm.* 3(5), 388-396. [Online]. Available: www.saspublisher.com
Rani, M., Agarwal, A., and Negi, Y. S. (2011). "Characterization and biodegradation studies for interpenetrating polymeric network (IPN) of chitosan-amino acid beads," *J. Biomater. Nanobiotechnol.* 2(1), 71-84. https://doi.org/10.4236/jbnb.2011.21010
Sapuła, P., Bialik-Wąs, K., and Malarz, K. (2023). "Are natural compounds a promising alternative to synthetic crosslinking agents in the preparation of hydrogels?" *Pharmaceutics* 15(1), article 253. https://doi.org/10.3390/pharmaceutics15010253
Sarhan, N., Arafa, E. G., Elgedawy, N., Elsayed, K. N. M., and Mohamed, F. (2024). "Urea intercalated encapsulated microalgae composite hydrogels for slow-release fertilizers," *Sci. Rep.* 14(1). https://doi.org/10.1038/s41598-024-58875-1
van Soest, J. J. G., Tournois, H., de Wit, D., and Vliegenthart, J. F. G. (1995). "Short-range structure in (partially) crystalline potato starch determined with attenuated total reflectance Fourier-transform IR spectroscopy," *Carbohydr. Res.* 279, 201-214.
Sringam, J., Pankongadisak, P., Trongsatitkul, T., and Suppakarn, N. (2022). "Improving

mechanical properties of starch-based hydrogels using double network strategy," *Polymers (Basel)* 14(17), article 3352. https://doi.org/10.3390/polym14173552

Sun, S.-W., Lin, Y.-C., Weng, Y.-M., and Chen, M.-J. (2006). "Efficiency improvements on ninhydrin method for amino acid quantification," *J. Food Compos. Anal.* 19(1), 112-117. https://doi.org/10.1016/j.jfca.2005.04.006

Tester, R. F., Karkalas, J., and Qi, X. (2004). "Starch-composition, fine structure and architecture," *Journal of Cereal Science* 39(2), 151-165. https://doi.org/10.1016/j.jcs.2003.12.001

Tomadoni, B., Casalongué, C., and Alvarez, V. A. (2019). "Biopolymer-based hydrogels for agriculture applications: Swelling behavior and slow release of agrochemicals," in: *Polymers for Agri-Food Applications*, Springer International Publishing, Cham, Switzerland, pp. 99-126. https://doi.org/10.1007/978-3-030-19416-1_7

Weiss, I. M., Muth, C., Drumm, R., and Kirchner, H. O. K. (2018). "Thermal decomposition of the amino acids glycine, cysteine, aspartic acid, asparagine, glutamic acid, glutamine, arginine and histidine," *BMC Biophys.* 11(1). https://doi.org/10.1186/s13628-018-0042-4

Wu, Y., Joseph, S., and Aluru, N. R. (2009). "Effect of crosslinking on the diffusion of water, ions, and small molecules in hydrogels," *J. Phys. Chem. B* 113(11), 3512-3520. https://doi.org/10.1021/jp808145x

Zhu, W., Long, J., and Shi, M. (2023). "Release kinetics model fitting of drugs with different structures from viscose fabric," *Materials* 16(8), 3282. https://doi.org/10.3390/ma16083282

Article submitted: July 21, 2025; Peer review completed: August 16, 2025; Revised version received: September 2, 2025; Accepted: November 4, 2025; Published: December 3, 2025.
DOI: 10.15376/biores.21.1.580-605

APPENDIX

Quantification of Aldehydes Groups

To determine the number of aldehydes groups in the filtrate, the colorimetric method was used (Boratynski and Zal 1990). A calibration curve was prepared with known concentrations of glutaraldehyde from 0.5 to 2 mM, from a stock solution of 0.01 M glutaraldehyde. From these solutions, 0.5 mL was extracted and reacted with 5 mL of *reagent 1* (40 µL of 5% phenol in 10 mL of 70% perchloric acid) for 30 min in a dark place, and the concentration was determined using the calibration curve (Fig. S1).

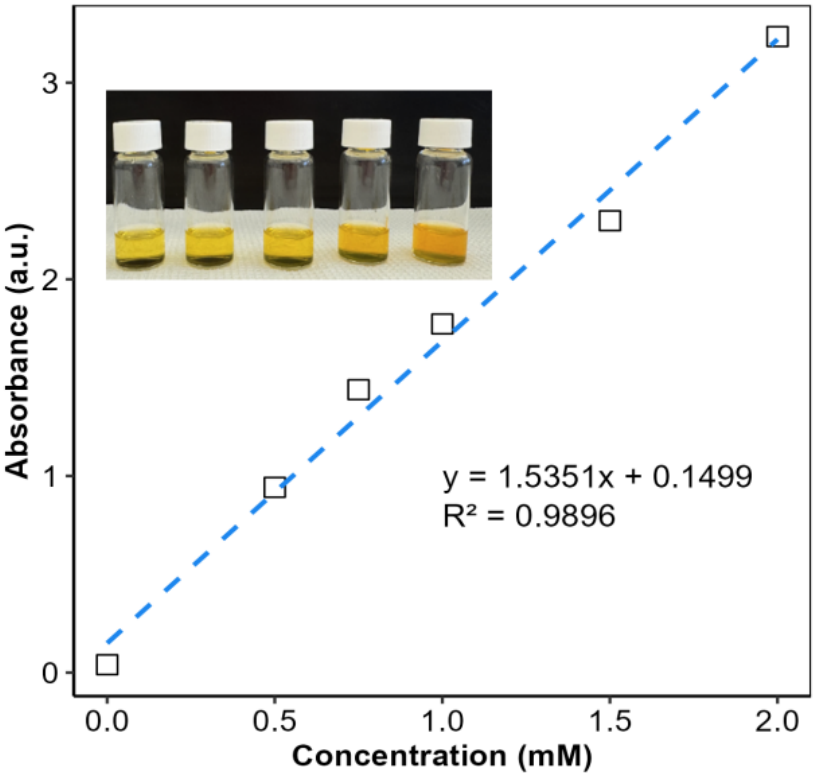

Fig. S1. Calibration curve obtained from standard solutions in the concentration range of 0.5 to 2 mM

Quantification of Amino Groups

To determine the quantity of primary amino groups in the filtrate, a protocol adapted from the Sun *et al.* (2006) was used. A calibration curve was prepared using a 0.01 M glycine stock solution. From this, solutions with a concentration range of 0.5 mM to 2 mM were prepared. According to Sun *et al.* (2006), when 1 mL of glycine solution is mixed with 2 mL of the *ninhydrin reagent* (0.2 g ninhydrin in 10 mL ethanol + 15 ml acetate buffer) and heated at 90 °C for 10 to 15 min, a purple solution is obtained. The absorbance is measured at a wavelength of 570 nm using a double-beam UV spectrometer (Agilent Cary 60 UV-Vis). The acetate buffer (0.2M, pH 5.5) was prepared by dissolving 16.4 g sodium acetate anhydrous per liter of deionized water and adjusting the pH to 5.5 with glacial acetic acid. The quantity of glycine in the filtrate was detected using a calibration curve (Fig. 2).

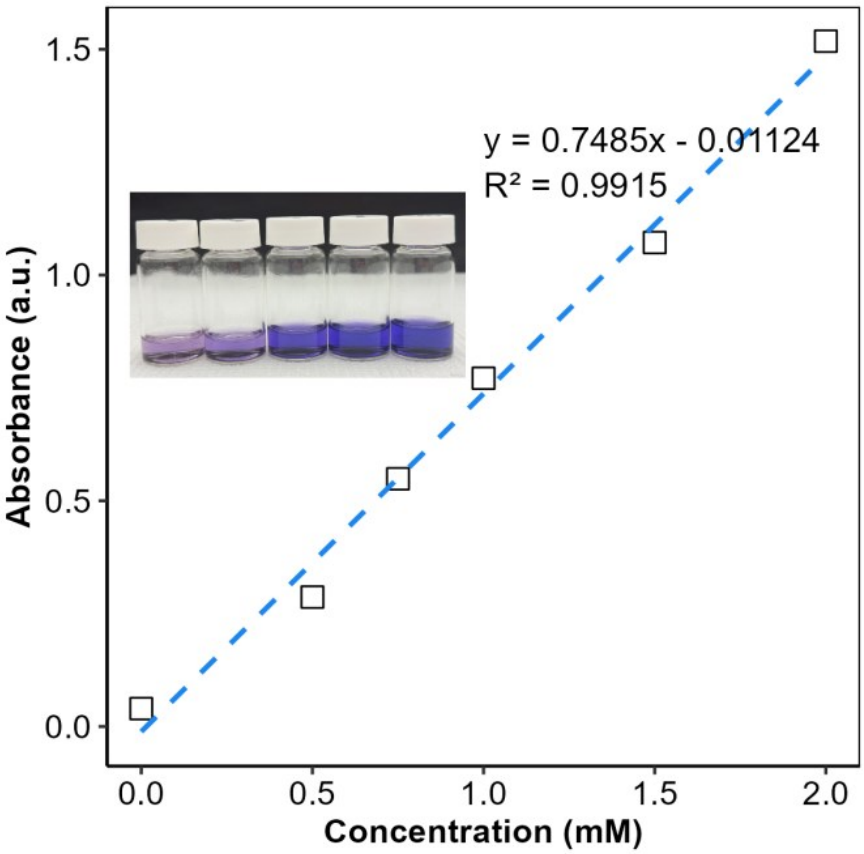

Fig. S2. Calibration curve obtained from standard solutions in the concentration range of 0.5 to 2 mM